Indonesian Journal of Informatics Education

Research Paper ISSN: 2549-0389

A Comparative Study of Digital Image Segmentation Algorithms for Acute Myeloid Leukemia M1 White Blood Cells Images

Nurcahya Pradana Taufik Prakisya
Informatics and Computer Engineering Education
Faculty of Teacher Training and Education,
Sebelas Maret University
nurcahya.ptp@staff.uns.ac.id

Andika Setiawan
Informatics Engineering
Department of Electro, Informatics and Physical System
Sumatera Institute of Technology
andika.setiawan@if.itera.ac.id

Abstract:

Various types of algorithms have been widely used for image segmentation in digital image processing. Every algorithm has features that make it unique to be applied to specific cases. One of the applications of image segmentation is to detect white blood cells. Certain objects such as blood cells must be able to be well segmented because their existence is very crucial to support the accuracy of disease detection related to haematology or the branch of medical science that studies the morphology of blood and blood-forming tissues. Three image segmentation algorithms were compared through this study: Seed Region Growing, Otsu Thresholding and Active Contour Without Edge. Comparative analysis of the three algorithms was done by counting the number of white blood cell objects that were successfully segmented with the actual number of cells that were counted manually. A total of 30 images of blood smears were taken from people suffering from acute myeloid leukemia M1. The average accuracy values from each algorithm were used to determine which image segmentation algorithm is the most suitable for application in the case of white blood cells segmentation. The results showed that Active Contour Without Edge is the most appropriate among the other algorithms.

Keywords: Acute Myeloid Leukemia, Active Contour Without Edge, Otsu Thresholding, Seed Region Growing.

Introduction

Utilization of image pattern recognition techniques in the medical world is currently being used intensively. Of course the pattern recognition technique does not stand alone, yet consists of several stages that actually play an important role in determining the success of the pattern recognition (Vaishnnave, Suganya Devi, Srinivasan, & Arutperumjothi, 2019). The image preprocessing stage, the stage of preparing image objects to be subjected to feature extraction and parameter calculation, is a very crucial step in a pattern recognition system. The accuracy of the object segmentation results from a method to ground truth makes it feasible to be used in a particular case (Suryani, Wiharto, Palgunadi, & Prakisya, 2017),

Leukemia or which can be called blood cancer is a dangerous disease that attacks the human body due to the uncontrolled growth of white blood cells (Sachin & Kumar, 2017). Bone marrow works continuously to form excess blood cells. The white blood cells formed from these blast cells are immature or abnormal so they cannot carry out their function as antibodies and result in reduced immunity in the human body (Setiawan et al., 2018). This disproportionate ratio of red blood cells and white blood cells makes the performance of blood as a medium for transporting nutrients and oxygen unable to run properly. Inappropriate identification and treatment that is not in accordance with the type of leukemia can have a negative impact and lead to death (Chen et al., 2019).

Leukemia is divided into four types: Acute Myeloid Leukemia (AML), Acute Lymphocytic Leukemia (ALL), Chronic Myeloid Leukemia (CML) and Chronic Lymphocytic Leukemia (CLL) (Harjoko et al., 2018). Leukemia M1 is a variant that originates from the myeloid predecessor and is so aggressive that it is referred to as acute myeloid leukemia (AML). The characteristics of AML M1 sufferers are the percentage of the number of myeloblasts in the blood by 90% of all non erythrites. The remaining percentage of white blood cells, promyelocyte, segment or monoblast cells, should be less than 10% (Bell & Sallah, 2005).

People with AML M1, if not treated immediately, can cause death in a matter of weeks or even days. Therefore, the use of digital image pattern recognition in leukemia is applied to assist pathologists in accelerating the process of identifying immature white blood cells. (Rajpurohit, Patil, Choudhary, Gavasane, & Kosamkar, 2018). Several studies in the field of computer vision apply various segmentation algorithms for leukemia cases. Separation between white blood cells (foreground) with blood plasma and red blood cells (background) needs to be done carefully so as to produce high accuracy. As for the challenge that often arises is that the objects of blood cells are overlapping so that they cannot be detected (overlapping) (Devi, Roy, Sharma, & Laskar, 2016). Object partial loss of white blood cells during the segmentation process can result in impairment of the accuracy of the identification of the type of white blood cells as well as the type of disease.

This research compares several image segmentation algorithms that are appropriate for use in image of blood preparations, namely: *seed region growing*, *otsu thresholding*, and *active contour without edge*. These three algorithms select white blood cells in a set of images of blood preparations from a person with AML M1. Several image preprocessing methods such as median filtering, opening, closing and color correction are necessary to make the images segmented-ready. The segmentation results in the form of binary white blood cell counts are then compared with the number of manual calculations. From a number of images, the average accuracy is sought. The algorithm with the best value of accuracy will be selected as the most appropriate algorithm to be used in further haematological research.

Related Work

Research related to object segmentation of white blood cells had been conducted by Prakisya, which used the seed region growing to separate a single object of white blood cells from its background. (Prakisya, Esti, & Wiharto, 2013). It was done by combining digital image processing with artificial neural network for the leukocyte types classification process. From 156 images with single object white blood cells, 151 of them were successfully segmented properly.

The otsu thresholding algorithm had been used by Suryani for blood cell segmentation in thalassemia betha mayor anemia (Suryani, Wiharto, & Wahyudiani, 2016). The blood cell images were normalized by changing the RGB color domain to YCbCr. This study applied a combination of color thresholding, otsu

thresholding and image morphology operations. The test results showed that the image morphology was able to identify Thalasemia Betha (β) Mayor Anemia.

Image segmentation algorithm using Active Contour Without Edge (ACWE) had also been used in a study related to blood morphology. Research conducted by Harjoko made the selection of white blood cells, red blood cells and several other artifacts in the blood preparations using inner energy and outer energy calculations from ACWE. Furthermore, each white blood cell object obtained was classified into four classes using momentum backpropagation. Five times testing calibration with the best parameter generated averages value of 84.754% precision, 75.887% sensitivity, 95.090% specificity and 93.569% accuracy (Harjoko et al., 2018).

Research Method

Comparison of the three image segmentation algorithms is not immediately possible. There are a series of stages that must be completed first. This research starts from the data acquisition stage, followed by image preprocessing, segmentation using the three algorithms, comparison of results and closed with drawing conclusions. The sequence of the research process can be shown in Figure 1.

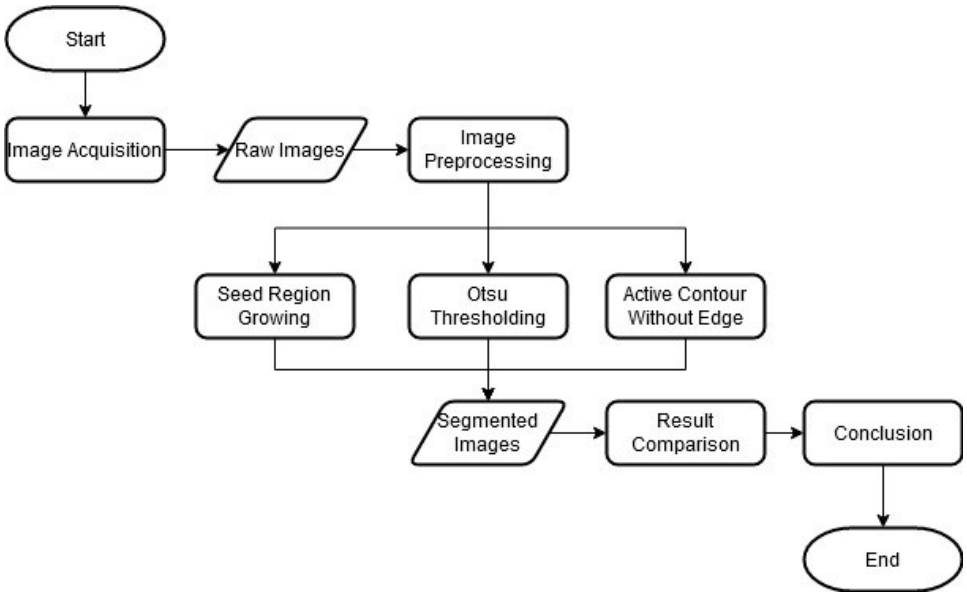

Figure 1. Research flow diagram

Image Acquisition

This process aims to collect data that were used in the segmentation process. The data used were camera-captured images of blood smear from a patient with leukemia M1. 30 images were selected selectively to represent the condition of M1 leukemia sufferers. This data is a dataset owned by Harjoko, et. al obtained from dr. Sardjito Hospital, Yogyakarta. A sample microscopic image of blood smear used for this research can be shown in figure 2.

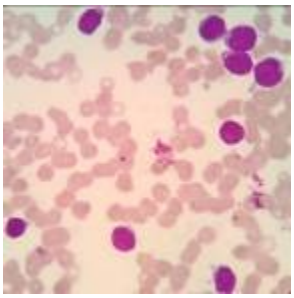

Figure 2. Blood smear image of leukemia M1

Image Preprocessing

The image preprocessing stage consists of a series of processes. It was started with noise reduction using median filtering. Median Filtering is effective in removing noise in the image by mediating on neighboring color pixels (Tong, Shi, Wu, Jiang, & Yang, 2018). Figure 3 shows a result of median filtering on blood smear image.

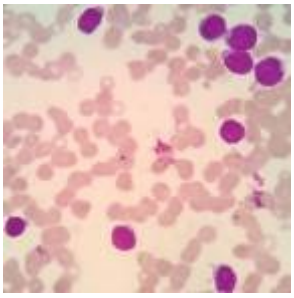

Figure 3. Median filtered image

Furthermore, the image color domain was changed to grayscale and adjusted so that the contrast between objects is clear. This contrast adjustment was applied using the equalization histogram (Shaikh Mohammed Bilal & Deshpande, 2018). After all processes were completed, image segmentation might begin. An image of segmentation-ready is shown in figure 4.

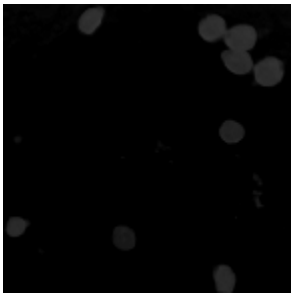

Figure 4. Preprocessed image

Seed Region Growing

Seed Region Growing (SRG) segmentation is an image segmentation method that uses region-based techniques. Pixels that are close together in the same area have the same visual features such as gray level, color value, or texture. The principle of the SRG is to start with the determination of seed points. From these seeds, areas will be grown with the addition of each seed where neighboring pixels have similar characteristics to it. If the seed is known, SRG will try to find accurate objects to be segmented from the area with the property where each component of the area that is connected to one of the seeds (Prakisya et al., 2013).

Woods and Gonzales (Gonzalez & Woods, 2008) stated that segmentation approach with a region growing algorithm based on an analysis of eight side by side pixels (8 connectivity), namely: If f (x, y) is the input pixel of an image; S (x, y) is the seed pixel and Q is the assessment criterion, so the region growing process runs as follows:

1. From the seed pixel S (x, y) find another 8 connected pixels.
2. Analyze all eight adjacent pixels based on predefined Q criteria. If any adjoining pixels meet the Q criterion, label the pixel 1. On the other hand, pixels that do not meet the criteria are labeled 0.
3. Save the pixel labeled 1 in the output image as a region.
4. In the f (x, y) image, find the pixel labeled 0 and perform the analysis as in points 2 and 3.
5. Carry out the process until all pixels in the f (x, y) image have been analyzed

The process of region growing can be shown in Figure 5. The process begins at a seed pixel as shown in Figure 5 (a). Figure 5 (b) shows the results of region growing after two iterations. The pixels with shading

are the pixels that are being analyzed. The region growing algorithm provides flexibility in determining and changing the criteria or Q value.

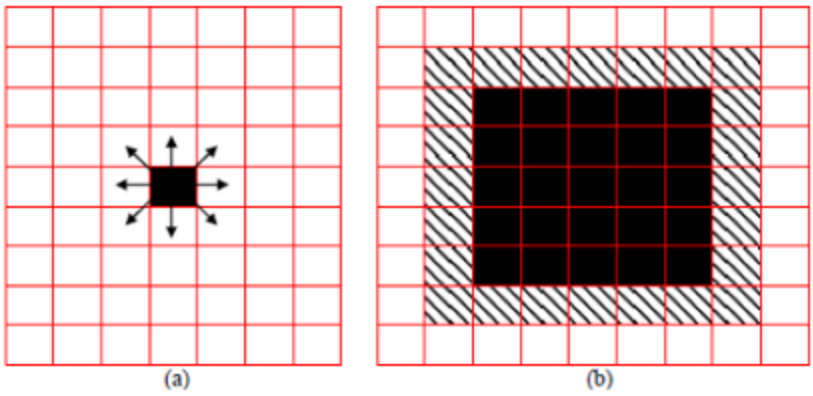

Figure 5. Seed Region Growing

The advantage of changing this Q value is that it can remove isolated pixels which are noises so that the segmentation results are more optimal. Thus, this algorithm is preferable to be applied to images that have high noise. But on the other hand, this algorithm requires a longer processing time because it has to perform operations on each pixel in the image (Mulkal, 2016).

Otsu Thresholding

Otsu Thresholding is a modification of the global thresholding method. It can automatically divide the gray level image histogram into two different areas without requiring user assistance to enter a threshold value. The approach is to perform discriminant analysis, namely determining a variable that can distinguish between two or more groups that arise naturally. Discriminant analysis will maximize these variables in order to divide the foreground and background objects so that the variance values of several segments of the image histogram are the same (Salat & Achmady, 2018).

The formula of the Otsu thresholding begins by finding the threshold value of a gray level image expressed by k. The value of k ranges from 1 to 255. The probability of each pixel at the i_{th} level can be stated:

$$P_i = n_i/N \qquad (1)$$

Where n_i is the number of pixels at level *i* and *N* is the total number of pixels in the image. The Zeroth cumulative moment, first cumulative moment, and total mean value respectively can be stated by the following formula

$$\omega(k) = \sum_{i=1}^{k} P_i \qquad (2)$$

$$\mu(k) = \sum_{i=1}^{k} i.P_i \qquad (3)$$

$$\mu_T = \sum_{i=1}^{L} i.P_i \qquad (4)$$

The k threshold value can be determined by minimizing the within class variance equation

$$\sigma_W^2(k^*) = \min_{1 \le k < L} \sigma_W^2(k)$$

$$\sigma_W^2(k) = W_b\sigma_b^2(k) + W_f\sigma_f^2(k) \qquad (5)$$

or also by maximizing the equation between class variance, which is as follows

$$\sigma_B^2(k^*) = \max_{1 \le k < L} \sigma_B^2(k)$$

$$\sigma_B^2(k) = \frac{[\mu_T \omega(k) - \mu(k)]^2}{\omega(k)[1-\omega(k)]} \qquad (6)$$

Active Contour Without Edge

The conventional active contour method uses the concept of an edge gradient to find the object so that it requires a large amount of energy in the segmentation process and uses the object edges defined by the image gradient to stop iterations. Therefore, the Active Contour Without Edge (ACWE) method was developed which minimizes the energy required and does not depend on the image gradient (Chan, Yezrielev Sandberg, & Vese, 2000)..

Basically ACWE makes a comparison between the total value of inside energy (F_1) and outside energy (F_2) as shown in the equation (7).

$$F_1(C) + F_2(C) = \int_{inside(C)} |u_0(x,y) - C_1|^2 dx\, dy + \int_{outside(C)} |u_0(x,y) - C_2|^2 dx\, dy \qquad (7)$$

The inside energy is the total square of the difference of each pixel that is scattered in the curve area with the mean of the pixels that are in the curve area (C_1). The outside energy is the total difference squared of each pixel that is spread outside the curve area with the mean of the pixels scattered outside the curve area (C_2) where $u_0(x,y)$represents the pixel value in the image *f (x, y)*. *C* is the variable of the curve where the values of C_1 and C_2 depend on the location of the pixel to the C curve in the image (Shah, Abaza, Ross, & Ammar, 2006). Let : ϕ be defined as a signed distance function from the curve C. Thus

$$C \subset \Omega \begin{cases} C = \partial\omega = \{(x,y) \in \Omega : \phi(x,y) = 0\}, \\ inside(C) = \omega = \{(x,y) \in \Omega : \phi(x,y) > 0\}, \\ outside(C) = \Omega/\bar{\omega} = \{(x,y) \in \Omega : \phi(x,y) < 0\} \end{cases} \qquad (8)$$

Ω is an image where C⊂Ω, ω⊂Ω, C⊂$\partial\omega$. ω represents the area of the object so that the inside (C) is the area ω, while outside (C) is the area Ω / $\bar{\omega}$. The F value which is the energy calculation is obtained from the calculation of the C curve will always evolve. The formula for the evolution of the F value can be shown in the equation (9).

$$F(C_1, C_2, C) = \mu . Length(C) + v . Area\left(inside(C)\right) + \lambda_1 \int_{insisde\,(C)} |(u_0(x,y) - C_1)|^2 dx\, dy + \lambda_2 \int_{outside\,(C)} |(u_0(x,y) - C_2)|^2 dx\, dy$$

(9)

Where λ_1, λ_2 are constants with value=1. The first term (kappa), is calculated as:

$$K = \frac{fxx.fy^2 - 2.fxy.fx.fy.fyy + fyy.fx^2}{fy^2 + fy^2 + \varepsilon^{1.5}} \qquad (10)$$

Kappa or curvature of the curve is the difference in the neighborliness of each pixel value based on ϕ of the image *f(x, y)*. The term curvature provides a smooth limitation on contour evolution by limiting the total contour. The second term, the term model misalignment, drives contour evolution. It measures the suitability of the model when the contour divides the image such that the mean intensity c1 and c2 have a maximum value. Thus, cutting edges are not required to support the algorithm.

Result Comparison

A total of 30 images of white blood cell preparations were subjected to the segmentation process with each algorithm so that at the end of this process there were 90 images resulting from those segmentations. A sample of fully segmented image can be shown in Figure 6.

Each result was count the number of objects that were successfully segmented and compared with the number of objects that were counted manually. This stage produced the accuracy value obtained through the formula.

$$accuracy = \frac{n_{counted} - |n_{segmented} - n_{counted}|}{n_{counted}} \quad (11)$$

Where $n_{segmented}$ is the number of white blood cell objects resulting from the segmentation process $n_{segmented}$ is the number of manually counted white blood cell objects.

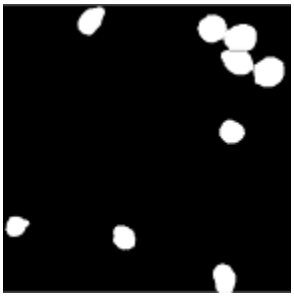

Figure 6. Fully segmented image

Conclusion Drawing

The compared results of the segmentation were selected the most appropriate to be applied to the image segmentation of white blood cells. Conclusion was based on the accuracy value obtained from each segmentation algorithm. The average of the greatest accuracy value indicates that the corresponding algorithm is the most appropriate algorithm. In research related to image processing on white blood cell images, it is suggested to use the selected segmentation algorithm.

Result and Analysis

Result

In the implementation of image segmentation, it is carried out in parallel. An image that is ready to be segmented is copied directly to each algorithm for treatment. There are 30 original images used for observation so that the total segmentation results are three times more, or 90 images. The figures below are examples of the segmentation results of each algorithm. A sample source image is shown in Figure 7(a). The result generated by seed region growing segmentation is shown in Figure (b). Figure 7 (c) shows the image segmented by otsu thresholding and figure 7 (d) shows the image segmented by active contour without edge.

Through the image example above, it appears that the image segmentation results using the seed region growing are more influenced by color uniformity. Each color that is within its tolerance range can become a seed and develop according to the calculation of region growing. The tolerance value of the red color used was 147 to 170. The green channel tolerance value was 32 to 40. The blue channel tolerance value was 130 to 142.

In the image segmented with otsu thresholding, the result was quite good, it's just that when the process was finding the right threshold point, there were still disturbing factors. One of which was the similarity of the pixel value in the grayscale image. The other one was some noise that came from artifacts that the median filtering cannot remove.

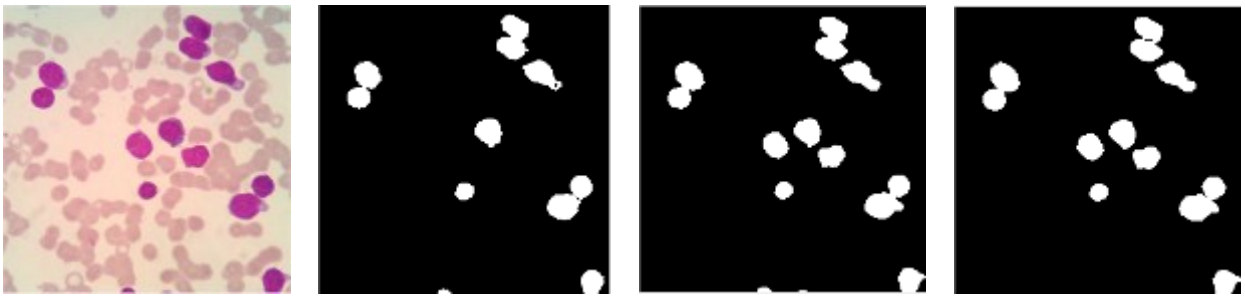

(a) (b) (c) (d)

Figure 7. Source image (a) and image segmented by (b) Seed Region Growing (c) Otsu Thresholding (d) Active Contour Without Edge

The segmented image with active contour without edge achieves stunning results. The white blood cell objects can be separated properly even if there is noise arising from the blood artifact. The calculation of internal energy and external energy makes the curve adaptable to the object in question. However, there are still some objects that were mis-segmented, including white blood cells that were cut off by the edges of the image but were still included in the calculation.

By using Equation 11, the accuracy values from three image segmentation algorithms in every single image were able to be acquired. For example, the cell count in Figure 7(b) is 11, the number of cells segmented with the otsu thresholding in Figure 7(c) is 13, and the amount of ACWE segmented cells in Figure 7(d) is 12. Meanwhile, the actual number of objects that can be counted on the original image is 12. Therefore, the accuracy values for the three algorithms are 91.3%, 91.3% and 100%, respectively. The rest of the results can be seen in Table 1.

Table 1. The results of white blood cells segmentation

Image	Manual Counting	Seed Region Growing	Otsu Thresholding	Active Contour Without Edge
Image 1	8	0 (0%)	9 (87.5%)	8 (100%)
Image 2	12	7 (58.3%)	12 (100%)	12 (100%)
Image 3	10	7 (70%)	12 (80%)	11 (90%)
Image 4	9	3 (33.3%)	10 (88.9%)	9 (100%)
Image 5	7	4 (57.1%)	7 (100%)	7 (100%)
Image 6	7	4 (57.1%)	9 (71.4%)	11 (42.8%)
Image 7	9	2 (22.2%)	10 (88.9%)	9 (100%)
Image 8	8	4 (50%)	11 (62.5%)	8 (100%)
Image 9	6	7 (83.3%)	9 (50%)	8 (66.7%)
Image 10	7	0 (0%)	10 (57.1%)	10 (57.1%)
Image 11	7	5 (71.4%)	8 (85.7%)	7 (100%)
Image 12	8	5 (62.5%)	8 (100%)	8 (100%)
Image 13	7	5 (71.4%)	8 (85.7%)	7 (100%)
Image 14	7	6 (85.7%)	9 (71.4%)	9 (71.4%)
Image 15	12	11 (91.3%)	13 (91.3%)	12 (100%)
Image 16	6	3 (50%)	6 (100%)	6 (100%)
Image 17	6	1 (16.7%)	7 (83.3%)	5 (83.3%)
Image 18	5	0 (0%)	5 (100%)	6 (80%)
Image 19	7	5 (71.4%)	8 (85.7%)	7 (100%)
Image 20	9	6 (66.7%)	9 (100%)	9 (100%)
Image 21	6	2 (33.3%)	6 (100%)	9 (50%)
Image 22	7	5 (71.4%)	7 (100%)	7 (100%)
Image 23	11	5 (45.5%)	11 (100%)	11 (100%)
Image 24	7	1 (14.3%)	7 (100%)	7 (100%)
Image 25	12	2 (16.7%)	13 (91.7%)	12 (100%)

Image 26	11	0 (0%)	11 (100%)	11 (100%)
Image 27	11	2 (18.2%)	13 (81.8)	11 (100%)
Image 28	10	3 (30%)	10 (100%)	9 (90%)
Image 29	4	1 (25%)	6 (50%)	4 (100%)
Image 30	9	4 (44.4%)	10 (88.9%)	10 (88.9%)
Average		**43.92%**	**86.74%**	**90.67%**

Analysis

The white blood cell object from each image that had been successfully separated by the segmentation algorithm was then calculated for its accuracy. Accuracy is calculated as a percentage by using equation 1. After obtaining all the values, the average accuracy was calculated. From table 1, it is known that the accuracy obtained by the seed region growing is 43.92%. The average value obtained is small because the color range used cannot accommodate the color variations that may occur in each white blood cell object

Meanwhile, the average accuracy value obtained by the otsu thresholding increased significantly to 86.74%, The contrast between background and foreground is quite good thanks to histogram equalization. This made it easier for the otsu thresholding to separate the white blood cells.

The active contour without edge algorithm successfully obtained 90.67%, a superior average accuracy value compared to the others. This average value indicates that the accuracy of the active contour without edge algorithm is the highest thus this algorithm is very feasible. for use in image segmentation of white blood cells.

Conclusion

Each image segmentation algorithm has its own advantages so that it can be applied to the right cases. In image segmentation with the aim of separating the white blood cell objects in the blood smear image, Active Contour Without Edge is more appropriate than the seed region growing and the otsu thresholding. It is proved by the comparison of the accuracy of the number of white blood cells which was successfully separated from 30 images by the three algorithms. The active contour without edge algorithm obtained 90.67% average value of accuracy which is greater than the seed region growing and the otsu thresholding, In the next study, which raised the theme of image segmentation of white blood cells, it would be better if it used the active contour without edge algorithm. However, the combination with multiple otsu thresholding or other segmentation methods can also be applied considering the accuracy value from the active contour without edge itself can still be improved

Acknowledgement (Optional)

We would like to thank dr. Sardjito Hospital Yogyakarta and Harjoko,et.al for the permission to use the set of Acute Myeloid Leukemia: M1 images.

References

Bell, A., & Sallah, S. (n.d.). *Bell & Sallah, 2005.pdf* (7th ed.). Abbott. A Promise for Life.

Chan, T. F., Yezrielev Sandberg, B., & Vese, L. A. (2000). Active contours without edges for vector-valued images. *Journal of Visual Communication and Image Representation*, *11*(2), 130–141. https://doi.org/10.1006/jvci.1999.0442

Chen, X., Pan, J., Wang, S., Hong, S., Hong, S., & He, S. (2019). The epidemiological trend of acute myeloid leukemia in childhood: A population-based analysis. *Journal of Cancer*, *10*(20), 4824–4835. https://doi.org/10.7150/jca.32326

Devi, S. S., Roy, A., Sharma, M., & Laskar, R. H. (2016). kNN Classification Based Erythrocyte Separation in Microscopic Images of Thin Blood Smear. *Proceedings - International Conference on Computational Intelligence and Networks*, *2016-Janua*, 69–72. https://doi.org/10.1109/CINE.2016.19

Gonzalez, R. C., & Woods, R. E. (2008). *Digital Image Processing Third Edition* (Third Edit). Prentice Hall,

Pearson.

Harjoko, A., Ratnaningsih, T., Suryani, E., Wiharto, Palgunadi, S., & Prakisya, N. P. T. (2018). Classification of acute myeloid leukemia subtypes M1, M2 and M3 using active contour without edge segmentation and momentum backpropagation artificial neural network. *MATEC Web of Conferences*, *154*. https://doi.org/10.1051/matecconf/201815401041

Mulkal. (n.d.). Implementasi Algoritma Region Growing untuk Segmentasi Retakan Bidang Batuan. *Implementasi Algoritma Region Growing Untuk Segmentasi Retakan Bidang Batuan*, (7).

Prakisya, N. P. T., Esti, S., & Wiharto. (2013). *Pemanfaatan Seed Region Growing Segmentation dan Momentum Backpropagation Neural Network untuk Klasifikasi Jenis Sel Darah Putih*. (May), 1–11.

Rajpurohit, S., Patil, S., Choudhary, N., Gavasane, S., & Kosamkar, P. (2018). Identification of Acute Lymphoblastic Leukemia in Microscopic Blood Image Using Image Processing and Machine Learning Algorithms. *2018 International Conference on Advances in Computing, Communications and Informatics, ICACCI 2018*, (Cll), 2359–2363. https://doi.org/10.1109/ICACCI.2018.8554576

Sachin, P., & Kumar, R. Y. (2017). Detection and Classification of Blood Cancer from Microscopic Cell Images Using SVM KNN and NN Classifier. *International Journal of Advance Research*, *3*(6), 315–324. Retrieved from www.ijariit.com

Salat, J., & Achmady, S. (2018). Minimalisasi Distorsi Dari Segmentasi Citra Metode Otsu Menggunakan Fuzzy Clustering. *ILKOM Jurnal Ilmiah*, *10*(1), 80–85. https://doi.org/10.33096/ilkom.v10i1.234.80-85

Setiawan, A., Harjoko, A., Ratnaningsih, T., Suryani, E., Wiharto, & Palgunadi, S. (2018). Classification of cell types in Acute Myeloid Leukemia (AML) of M4, M5 and M7 subtypes with support vector machine classifier. *2018 International Conference on Information and Communications Technology, ICOIACT 2018*, *2018-Janua*(Cml), 45–49. https://doi.org/10.1109/ICOIACT.2018.8350822

Shah, S., Abaza, A., Ross, A., & Ammar, H. (2006). AUTOMATIC TOOTH SEGMENTATION USING ACTIVE CONTOUR WITHOUT EDGES. *2006 Biometrics Symposium*, 0–5.

Shaikh Mohammed Bilal, N., & Deshpande, S. (2018). Computer aided leukemia detection using digital image processing techniques. *RTEICT 2017 - 2nd IEEE International Conference on Recent Trends in Electronics, Information and Communication Technology, Proceedings*, *2018-Janua*(1), 344–348. https://doi.org/10.1109/RTEICT.2017.8256613

Suryani, E., Wiharto, Palgunadi, S., & Prakisya, N. P. T. (2017). Classification of Acute Myelogenous Leukemia (AML M2 and AML M3) using Momentum Back Propagation from Watershed Distance Transform Segmented Images. *Journal of Physics: Conference Series*, *801*(1). https://doi.org/10.1088/1742-6596/801/1/012044

Suryani, E., Wiharto, W., & Wahyudiani, K. N. (2016). Identifikasi Anemia Thalasemia Betha (?) Mayor Berdasarkan Morfologi Sel Darah Merah. *Scientific Journal of Informatics*, *2*(1), 15–27. https://doi.org/10.15294/sji.v2i1.4525

Tong, J., Shi, H., Wu, C., Jiang, H., & Yang, T. (2018). Skewness correction and quality evaluation of plug seedling images based on Canny operator and Hough transform. *Computers and Electronics in Agriculture*. https://doi.org/10.1016/j.compag.2018.10.035

Vaishnnave, M. P., Suganya Devi, K., Srinivasan, P., & Arutperumjothi, G. (2019). Detection and classification of groundnut leaf diseases using KNN classifier. *2019 IEEE International Conference on System, Computation, Automation and Networking, ICSCAN 2019*, 1–5. https://doi.org/10.1109/ICSCAN.2019.8878733